Scientific paper

Enhanced Catalytic Degradation of Acid Orange 7 Dye by Peroxymonosulfate on Co_3O_4 Promoted by Bi_2O_3

Vanina Ivanova-Kolcheva,[1] Labrini Sygellou[2] and Maria Stoyanova[2,*]

[1] *Department of Physical Chemistry, University of Plovdiv 24, Tsar Asen Str., 4000 Plovdiv, Bulgaria*

[2] *Foundation for Research and Technology, Institute of Chemical Engineering Sciences (FORTH/ICE-HT), Patras, GR-26504, Greece*

** Corresponding author: E-mail: marianas@uni-plovdiv.bg*
tel: +35 932 261248 fax: +35 932 261403

Received: 10-16-2019

Abstract

In this study, Bi_2O_3-Co_3O_4 composite oxides were prepared and their catalytic efficiency to activate peroxymonosulfate (PMS) towards the degradation of Acid Orange 7 dye (AO7) was evaluated. The characterization of the synthesized catalysts was carried out by XRD, TEM, XPS, FT-IR, and ICP-OES analyses. The increased basicity of the Bi_2O_3-Co_3O_4 hybrids contributed to the much better catalytic activity in PMS activation resulting in a considerably higher rate of AO7 degradation compared to that obtained with bare Co_3O_4. The sample with 50 wt.% Bi_2O_3 showed the best performance under a broad pH range with very low Co leaching of 72 μg/L even under acidic conditions. Degradation of 50 mg/L AO7 reached almost 100% within a short duration of 12 min by using very low catalysts concentration of 0.1 g/L and [PMS]/[AO7] = 6. The influence of the Bi_2O_3 content, catalyst dosage, molar ratio of [PMS]/[AO7], initial pH, and temperature on AO7 degradation were studied. Surface-bound sulfate radicals generated in the Bi_2O_3-Co_3O_4/PMS oxidation system were proved as the predominant radical species through radical quenching experiments.

Keywords: Acid orange 7 degradation; Bi_2O_3-Co_3O_4 catalyst; peroxymonosulfate; sulfate radicals

1. Introduction

Azo dyes represent one of the largest groups of organic pollutants in wastewaters, generally released from textile, leather, paper, printing, plastic, food, pharmaceutical and cosmetic industries.[1,2] Dyes are not only highly visible, but also toxic, mutagenic, carcinogenic and low biodegradable.[3–5] Therefore, these contaminants must be removed from wastewater prior to discharge into natural water bodies to prevent their detrimental effect to the natural ecosystem and human health. Due to the complex aromatic molecular structures of azo dyes, most of them are persistent and recalcitrant in the environment and therefore cannot easily be degraded by the conventional wastewater treatment processes.[6–8] In the recent decade, the application of peroxymonosulfate (PMS) based catalytic oxidation processes for the degradation of several refractory organic contaminants in water including dyes has attracted increasing interest.[9–13] PMS is capable of generating highly reactive radicals, such as sulfate radicals ($SO_4^{\bullet-}$, E^o = 2.5–3.1 V) and hydroxyl radicals (•OH, E^o = 1.9–2.7 V), by activation through transition metals and their oxides,[9–16] ultrasound,[17,18] anions,[19,20] and base.[21,22] Compared to the •OH, $SO_4^{\bullet-}$ has a longer lifetime (30–40 ms vs 20 ns) thus allowing it to react effectively with the target organic pollutant.[23] Among the PMS activation methods, the most feasible route for production of $SO_4^{\bullet-}$ radicals is catalytic activation by transition metal ions, with cobalt ions (Co^{2+}) being the best activator.[14] Anipsitakis and Dionysiou showed that Co^{2+}/PMS could be an alternative method for degradation of organic compounds with excellent performance in neutral pH, which is an applicable benefit of this system compared to the Fenton reagent.[9] However, the difficult recovery of the homogeneous catalyst and especially the problem related to the potential environmental and health impact of cobalt in aquatic environment limit the practical-scale application of the homogeneous Co^{2+}/PMS system. Therefore, the development of

heterogeneous cobalt-based catalysts to activate PMS with low cobalt leaching is highly desirable. Among cobalt oxides, Co_3O_4 has been thoroughly investigated to activate PMS for degradation of various organic pollutants in water such as 2,4-dichlorophenol,[24] phenol,[25,26] antibiotics,[16,27] and dyes.[28,29] In order to enhance the catalytic performance and reduce cobalt leaching of Co_3O_4, several supports such as common oxide materials (Al_2O_3, TiO_2, MgO, SBA-15), activated carbon, carbon nanofibers, zeolite, etc. have been used for hosting Co_3O_4 particles and tested for oxidative degradation of contaminants in the presence of PMS.[10,30–35] Zhang et al. reported for a much better performance of Co/MgO catalyst than bulk Co_3O_4 for degradation of methylene blue dye via heterogeneous PMS activation.[30] The abundance of surface hydroxyl groups on the MgO support facilitate the formation of surface Co–OH complexes, which is considered as the rate-limiting step for PMS activation.[31] Co_3O_4 supported on graphene oxide was prepared and used in the degradation of azo dye AO7 by advanced oxidation technology based on sulfate radicals.[36] The Co_3O_4/GO nanocomposite exhibits a markedly better efficiency for PMS activation than both the homogeneous Co^{2+} and the heterogeneous unsupported Co_3O_4 catalyst due to the Co–OH complexes formed on the surface of the GO sheet through the direct interaction of Co species with nearby hydroxyl groups. As the presence of surface basic sites can promote the formation of the surface Co–OH complex, doping of Co_3O_4 with basic metal oxides would have a promotional effect on its PMS activation ability. Due to the high density of surface hydroxyl groups of the Bi-based materials, their synergistic coupling with Co_3O_4 can enhance its catalytic performance for PMS activation.[37] The bimetallic Co-Bi oxide catalyst synthesized using a microwave-assisted method showed a much higher bisphenol A degradation and TOC removal efficiency via PMS activation than those of Co_3O_4/PMS and Bi_2O_3/PMS systems.[38]

Herein, a performance evaluation of Bi_2O_3-Co_3O_4 catalysts as PMS activator for oxidative degradation of azo dye Acid Orange 7 is investigated. The kinetics of the oxidation process and the effects of various operational parameters, namely Bi_2O_3 content, catalyst dosage, molar ratio of [PMS]/[AO7], initial pH, and reaction temperature on the catalytic efficiencies in Bi_2O_3-Co_3O_4 /PMS system were studied in detail. Specific quenching studies were also carried out to identify the primary radical species formed from the catalyst-mediated decomposition of PMS.

2. Experimental

2. 1. Chemicals

Cobalt nitrate ($Co(NO_3)_2 \times 6H_2O$), bismuth nitrate ($Bi(NO_3)_3 \times 5H_2O$), magnesium nitrate ($Mg(NO_3)_2 \times 6H_2O$), Acid Orange 7 (AO7) and methylene blue (MB) were provided by Sigma-Aldrich (St. Louis, MO, USA). Oxone ($2KHSO_5 \cdot KHSO_4 \cdot K_2SO_4$, 4.7% active oxygen) was obtained from Sigma-Aldrich (St. Louis, MO, USA) and used as an oxidant. Other reagents were of analytical grade and were purchased as reagent grade. All chemicals were used as received without any further purification. Double distilled water was used to prepare solutions.

2. 2. Preparation of Bi_2O_3-Co_3O_4 Composite Catalysts

The x-Bi_2O_3-Co_3O_4 (x presenting the weight ratio of Bi_2O_3 to Bi_2O_3-Co_3O_4 composite, x = 20%, 50%, and 80%) were prepared by co-precipitation method and subsequent annealing of the co-precipitated precursors. For the co-precipitation process, 0.8 mol/L NaOH was added dropwise at 333 K into a solution of metal nitrates containing Co^{2+} and Bi^{3+}, taken in the specified stoichiometric ratio, under vigorous stirring until the solution pH reached 10. The initially formed precipitate was kept under continuous stirring for 30 minutes at 333 K. After filtration, the black product was washed with deionized water and ethanol several times to neutral pH, dried at 378 K overnight, and finally calcined at 773 K for 3 h in static air. For comparison, pristine Co_3O_4 and Bi_2O_3 were also prepared by the same synthetic procedure.

2. 3. Characterization

The Co and Bi contents in the composites as well as the concentration of leached Co ions after the reaction were determined by ICP-OES analysis on an iCAP 6300 instrument (ThermoFisher, MA, USA). The crystal structures of the synthesized catalysts were analyzed by X-ray diffraction. The powder XRD patterns were collected on a Bruker D8 Advance diffractometer (Bruker AXS, Billerica, MA, USA) equipped with Cu Kα radiation and LynxEye detector. Phase identification was performed with the Diffracplus EVA using ICDD-PDF2 Database. The morphology of the catalysts was characterized by a JEM 2100 high-resolution transmission electron microscope (JEOL, Tokyo, Japan) using an accelerating voltage of 200 kV. Two basic regimes of microscope mode were used – bright-field transmission microscopy (TEM) and selected area electron diffraction (SAED). The surface elemental composition and chemical oxidation state were investigated by an X-ray photoelectron spectroscopy (XPS) on a UHV chamber ($P < 10^{-9}$ mbar) equipped with a dual Mg/Al X-Ray gun and a SPECS LHS-10 hemispherical electron analyzer, using an MgKα ($h\nu$ = 1253.6 eV) X-ray source operated at 10 mA and 12 kV. The XPS spectra were analyzed with ECLIPSE using a Shirley background. The binding energies (BEs) obtained from the XPS analysis were calibrated with a reference BE of C 1s (284.8 eV). Fourier transform infrared (FT-IR) spectra were collected with a Vertex 70 spectrophotometer (Bruker Optics) using KBr pellets. The BET specific surface area of the samples was determined from the nitrogen adsorp-

tion-desorption using a Tristar 3000 porosimeter (Micromeritics, Aachen, Germany) at the liquid nitrogen temperature. The pH of the point of zero charge (pH_{PZC}) of the catalysts was determined by pH drift method.[39]

2. 4. Catalytic Degradation Procedure

Batch experiments were carried out in a 400 mL glass reactor with constant stirring at around 400 rpm at 293 K. Typically, a certain dose of solid PMS (in the form of Oxone, $2KHSO_5 \cdot KHSO_4 \cdot K_2SO_4$) was added into a 200 mL 50 mg/L AO7 aqueous solution to attain the predefined PMS/AO7 molar ratio and stirred until dissolved. Degradation reaction was initiated by addition of a specified amount of catalyst. At the given time intervals, 4.0 mL of suspension was taken and quenched by 1 mL methanol to stop the reaction, and then centrifuged at 4000 rpm for 1 min to remove the catalyst.

The concentration of AO7 was analyzed by UV–vis spectroscopy (Cintra 101, GBC Scientific Equipment Ltd., Australia) at a maximum wavelength of 486 nm. All tests were conducted in triplicate to ensure the reproducibility of experimental results. For the quenching experiments, prior to the addition of oxidant and catalyst, a specified amount of radical scavengers was added into the AO7 solution to obtain a required scavenger/PMS molar ratio.

3. Results and Discussion

3. 1. Characterization of Bi_2O_3-Co_3O_4 Catalysts

The Bi_2O_3 content in the synthesized composite materials calculated on the basis of ICP-OES results was close to preparation settings (25.7, 52.9, and 78.4 wt.% for the 20%, 50%, and 80% Bi_2O_3-Co_3O_4 samples, respectively).

The crystal structure of Bi_2O_3-Co_3O_4 catalysts was analyzed by XRD and compared to that of pure Bi_2O_3 and

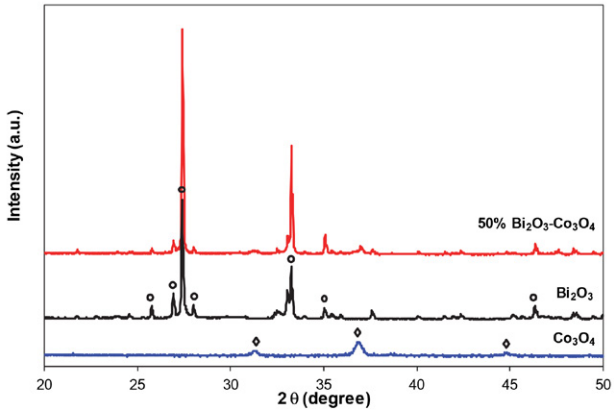

Fig. 1. XRD patterns of 50% Bi_2O_3-Co_3O_4, Co_3O_4, and Bi_2O_3

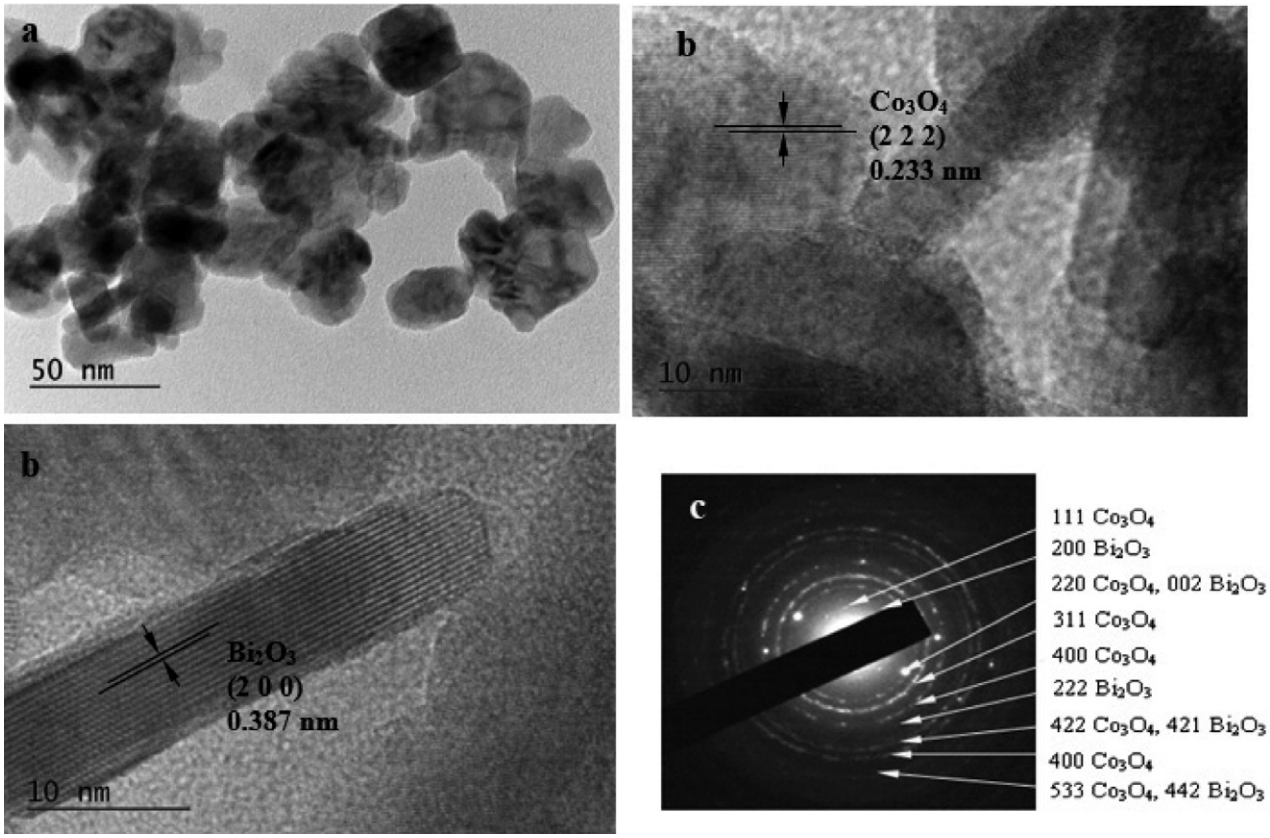

Fig. 2. (a) Bright-field TEM image, (b) HRTEM images and (c) SAED pattern of 50% Bi_2O_3-Co_3O_4.

Co_3O_4 (Fig. 1). The crystallographic phases of the prepared pristine oxides were confirmed as monoclinic α-Bi_2O_3, (JCPDS 41-1449) and cubic spinel-type Co_3O_4 (JCPDS 42-1467), respectively. For the composite catalysts, the characteristic peaks of Bi_2O_3 were observed at about 2 Θ values 26.93º (1 1 1), 27.40° (1 2 0) and 33.26° (2 0 0). The diffraction peaks at 31.2°, 36.9° and 44.7° can be indexed to (220), (311) and (400) planes of Co_3O_4 crystal (JCPDS 42-1467). As seen in Fig. 1, reflections associated with cobalt species in Bi_2O_3-Co_3O_4 were too weak, suggesting good dispersion of the Co_3O_4 particles in the resulting product. Moreover, no positive shift of the diffraction peaks of Bi_2O_3 was registered in the composite catalyst, which suggests that Co species are not incorporated into Bi_2O_3 lattice and Co_3O_4 and Bi_2O_3 coexist in the composite.

The coexistence of Co_3O_4 and Bi_2O_3 phases in the composite catalysts was confirmed through TEM and HR-TEM analysis. As observed in Fig. 2a, the 50 wt.% Bi_2O_3-Co_3O_4 sample was composed of predominantly flat particles with a near-rectangular shape and size in the range of 30–50 nm. The HRTEM image of the sample (Fig. 2b) showed well-defined lattice fringes, which indicates that it was highly crystallized. The fringes of d = 0.233 nm matched the (2 2 2) plane of Co_3O_4 nanoparticles, while the fringes of d = 0.387 nm corresponded to the (2 0 0) plane of α-Bi_2O_3, respectively. This confirmed that both Bi_2O_3 and Co_3O_4 phases coexisted in the Bi_2O_3-Co_3O_4 samples. The SAED pattern (Fig. 2c) obtained from the TEM showed well-defined rings and spots characteristic of well crystalline materials. Indexations of the diffraction pattern confirm the presence of both oxide phases in the catalyst.

The functional groups on the 50 wt.% Bi_2O_3-Co_3O_4 composite and bare Co_3O_4 and Bi_2O_3 were analyzed by FTIR technique and the obtained FTIR spectra are shown in Fig. 3. The formation of Co_3O_4 spinel oxide in the composite catalyst was confirmed by the presence of two distinct absorption bands at 573 and 665 cm^{-1} which originate from the stretching vibrations of the cobalt-oxygen bonds. The low frequency band represents the vibrations of octahedrally coordinated Co^{3+} with oxygen in the spinel lattice, while the high frequency band at 665 cm^{-1} can be assigned to the tetrahedral Co^{2+}.[37,40] The band at 847 cm^{-1} registered in the FTIR spectra of Bi_2O_3-Co_3O_4 and pure Bi_2O_3 is related to the vibration of Bi-O bonds and the existence of α-Bi_2O_3.[41] In all samples, the absorption peaks at around 3445 and 1630 cm^{-1} correspond to the stretching and bending vibrations of hydroxyl groups and the adsorbed water molecules, respectively.[42]

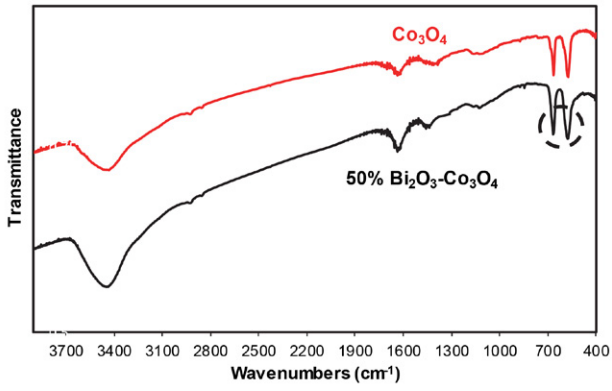

Fig. 3. FTIR spectra of the 50% Bi_2O_3-Co_3O_4, Co_3O_4 and Bi_2O_3

XPS measurements were conducted to elucidate the surface characteristics of the prepared composite catalysts. Obvious photoelectron peaks due to Co, Bi and O elements were detected in the survey spectrum of 50 wt.% Bi_2O_3-Co_3O_4 sample (Fig. 4a), confirming the presence of these elements on the surface of the catalyst. The curve fitting of Co 2p spectrum is shown in Fig. 4b. The Co 2p peaks at binding energies of 779.5 eV and 794.2 eV with satellite peak at 789.2 eV are characteristics of Co^{3+} located at octahedral sites in the cubic spinel structure of Co_3O_4, while the peaks at 781.4 eV and 796.4 eV with satellite signal at 787.7 eV are assigned to tetrahedral Co^{2+}. The calculated atomic ratio of Co^{3+} to Co^{2+} was 1.93, which is typical for Co_3O_4. The spin-orbit splitting of the Co $2p_{3/2}$ and Co $2p_{1/2}$ peaks signals was 15.1 eV, which is well consistent with the literature data of spinel Co_3O_4 and further confirmed that Co is present in the form of Co_3O_4 in composite catalysts.[43] Two evident peaks observed at 162.7 eV and 156.9 eV in Bi 4f XPS spectrum of (Fig. 4c) are assigned to Bi 4f 5/2 and Bi 4f 7/2 of Bi_2O_3, respectively.[44] The high-resolution XPS spectrum of O 1s (Fig. 4d) shows two different peaks at 529.7 and 531.5 eV, which were assigned to the lattice oxide oxygen and surface hydroxyl groups, respectively.[45] Quantitative analysis of the O 1s spectra reveals that the relative content of the surface hydroxyl oxygen in the Co-Bi composite (22% of the total oxygen) was twice higher than calculated for pure Co_3O_4. The availability of more hydroxyl groups on the surface of composite catalysts can promote the formation of surface Co-OH complexes, which may favour the enhancement of the catalytic activity of Co catalysts for PMS activation.

3. 2. Catalytic Performance of Bi_2O_3-Co_3O_4 /PMS System on AO7 Oxidative Degradation

The AO7 oxidative degradation was selected to evaluate the catalytic performance of the Co-Bi composite oxides for PMS activation. Initially, to confirm the occurrence of a catalytic reaction in the catalyst/PMS system, control experiments including adsorption tests and no catalyst addition were conducted. In comparison, the Co_3O_4, Bi_2O_3 and Co(II) ions (dissolved $Co(NO_3)_2$) were employed as references. Fig. 5 shows that no noticeable removal of AO7 was observed in the single use of PMS after 30 min, indicating that PMS alone cannot produce free radicals to induce AO7 degradation. The as-prepared composite catalyst had no obvious adsorption toward AO7

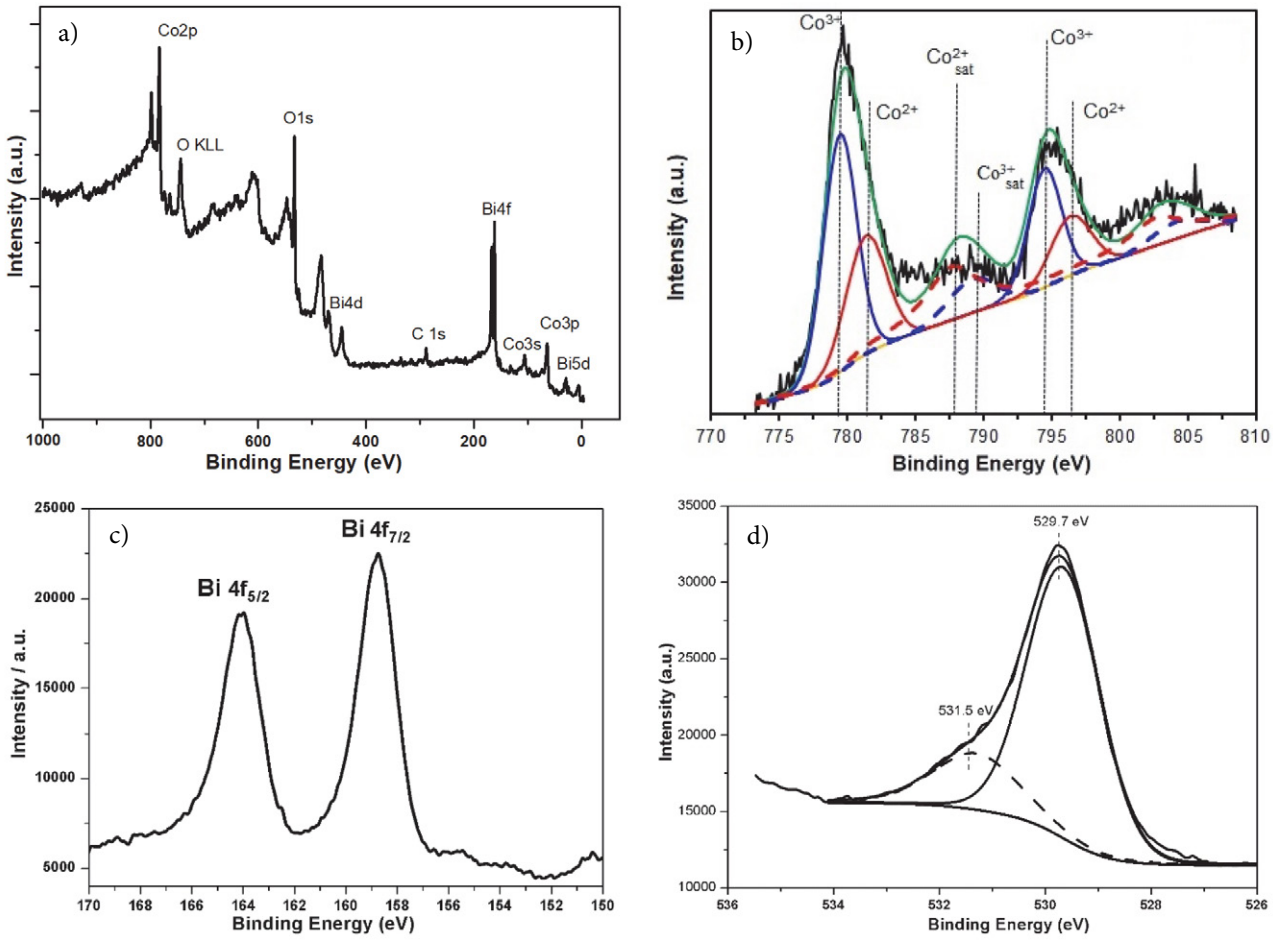

Fig. 4. XPS spectra of 50% Bi_2O_3-Co_3O_4 sample: (a) wide survey, (b) Co 2p, (c) Bi 4f and (d) O1s

and only less than 5% of the dye was removed in 30 min. PMS also did not cause any decrease in the AO7 concentration when it was combined with pristine Bi_2O_3, indicating that Bi_2O_3 had low reactivity for PMS activation to degrade the dye. When bare Co_3O_4 was used as the catalyst for the activation of PMS to generate the active radicals, only 39% decolorization efficiency could be achieved within 12 min, while a complete discoloration of the solution was attained for 90 min. However, doping of Bi_2O_3 on Co_3O_4 greatly improved its catalytic performance for PMS activation and catalytic degradation of AO7. Specifically, after the addition of PMS, AO7 was completely degraded in 12 min using Co_3O_4 doped with 50 wt.% Bi_2O_3, which should be attributed to the fast running radical-involved process. Since the contributions of adsorption and direct PMS oxidation on the AO7 removal are negligible, the catalytic oxidation over the composite catalyst can be considered as the main AO7 removal pathway. Furthermore, given that PMS is inefficient for AO7 degradation alone, the observed rapid first degradation stage in the degradation curve of 50% Bi_2O_3-Co_3O_4 indicates that a large number of free radicals are generated upon the contact of the oxidant with the catalyst surface.

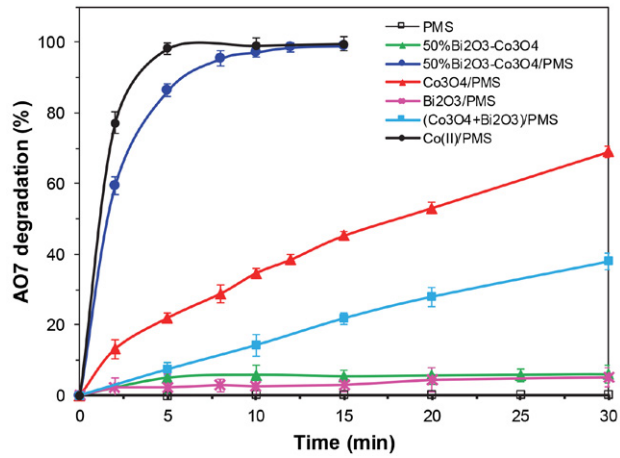

Fig. 5. Removal profiles of AO7 in different systems. Reaction conditions: $[AO7]_o$ = 50 mg/L; [PMS]/[AO7] = 6; [Catalyst]= 0.1 g/L; $[Co^{2+}]$ = 0.39 mg/L; initial pH = 3.04; T = 293 K.

The superior catalytic activity of Co-Bi composite oxides relative to either Co_3O_4 or Bi_2O_3 suggests a synergistic effect of both oxides in the catalysts towards PMS activation for AO7 degradation. This synergetic coupling

effect was further proved by degradation test conducted using the mechanical mixture of Co_3O_4 and Bi_2O_3 with a weight ratio of 1:1 as a catalyst. The results indicated that the catalytic performance of this mixture was evidently inferior to that of 50% Bi_2O_3-Co_3O_4 composite under identical conditions. In fact, only 22% AO7 removal in 15 min was achieved in the presence of the mechanical mixture, which is close to the average degradation value by Co_3O_4 and Bi_2O_3. Furthermore, a linear AO7 removal profile in a mechanical mixture/PMS system further evidences that activation of oxidant is the rate-limiting step of the oxidation process rather than the destruction of the dye molecules by radicals formed.

The catalytic performance of the most active composite 50% Bi_2O_3-Co_3O_4 was slightly inferior to the Co(II) ions, used as a homogeneous catalyst for the activation of PMS at the same molar concentration of the solid catalyst. It could be speculated that the high weight percent of cobalt oxide in the catalyst may lead to significant leaching of Co ions in the solution. However, though the leaching process occurred during the degradation reaction, the amount of dissolved Co ions was detected to be up to 72 μg/L (Co leaching percent of 0.21%) after the reaction was completed even in acidic conditions. This gives a reason to suggest that the homogeneous activation of PMS by leached Co(II) ions would be negligible and the heterogeneous pathway of PMS activation dominated in the Bi_2O_3-Co_3O_4/PMS system. The insignificant contribution of the homogeneous catalytic reaction promoted by dissolved Co ions was also confirmed by comparative experiments, in which leaching solution obtained upon complete removal of AO7 and filtering the catalyst was used to activate PMS for the oxidation of dye again. Less than 4% AO7 was degraded in the leaching solution by PMS addition, which was much lower compared to the Bi_2O_3-Co_3O_4/PMS oxidation system, indicating that the main catalytic contribution is from the composite catalyst, not dissolved cobalt ions.

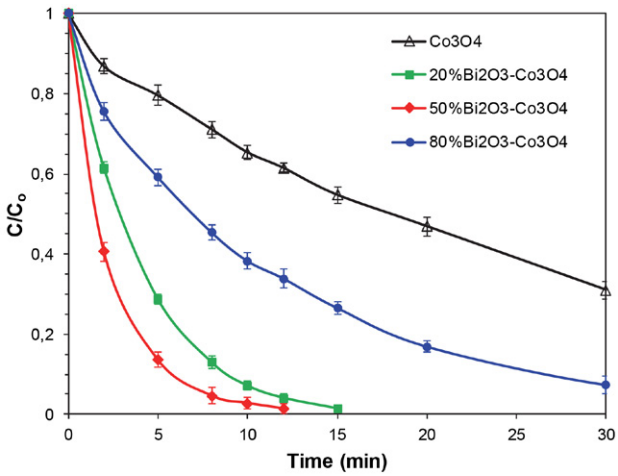

Fig. 6. AO7 catalytic degradation in x-Bi_2O_3-Co_3O_4 composite/PMS systems. Reaction conditions: $[AO7]_o$ = 50 mg/L; [PMS]/[AO7] = 6; [Catalyst]= 0.1 g/L; initial pH = 3.04; T = 293 K.

The Bi_2O_3 mass content in the composite catalysts had a noticeable influence on the catalytic activity of Co_3O_4 resulting in different AO7 degradation profiles. As seen from Fig. 6, the AO7 degradation efficiency considerably increased with the increase of Bi_2O_3 content up to 50%. However, as the Co_3O_4 particles in the composites determined the PMS activation, the excessive amount of Bi_2O_3 (80 wt.%) did not further promote the catalytic activity of Co_3O_4 and only 66% of dye was degraded for 12 min. Nevertheless, the catalytic efficiency of all Bi_2O_3-Co_3O_4 composites was higher than that of bare Co_3O_4.

Data of AO7 degradation with various catalysts in the PMS oxidation system were fitted well with the pseudo-first-order kinetic model (Fig. 7), indicating that the catalytic process is not controlled by the PMS activation step and radical generation. As seen from the inserted figure, the reaction rate constant (k) of AO7 degradation increased considerably upon doping of Co_3O_4 with Bi_2O_3, demonstrating the positive effect of Bi_2O_3 addition for the faster PMS activation. Specifically, the kinetic constant for 50% Bi_2O_3-Co_3O_4 is *ca.* 9.5 times higher than those of Co_3O_4 although the specific surface area of the composite (28.12 m^2/g) was only slightly lower than that of the pure cobalt oxide (30.1 m^2/g). This result indicates that some other factors besides the specific surface area played much more important roles in the activation process.

The much better performance for PMS activation ex-

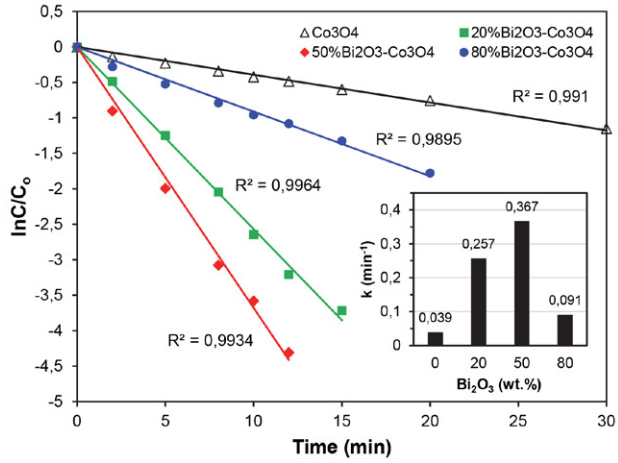

Fig. 7. First-order kinetic fitting of the AO7 degradation curves. Reaction conditions: $[AO7]_o$ = 50 mg/L; [PMS]/[AO7] = 6; [Catalyst] = 0.1 g/L; initial pH = 3.04; T = 293 K.

hibited by Bi_2O_3-Co_3O_4 hybrids than the bare cobalt oxide could be attributed to the increased basicity of the Co_3O_4 surface after Bi_2O_3 modification resulting in a more hydroxylated surface that facilitates the decomposition of PMS to reactive radicals. This suggestion was well in accordance with the point of zero charge (pH_{pzc}) measurements. The pH at which the curve pH(final) = pH(initial) crosses the dashed line, obtained without the addition of a catalyst (see Fig. 8) is taken as the pH_{pzc} of the given cata-

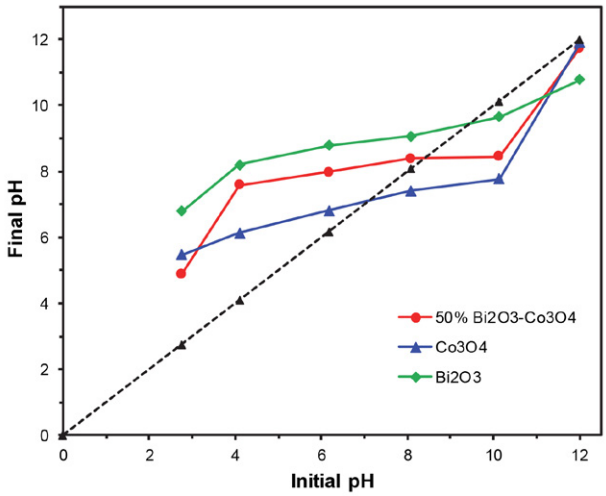

Fig. 8. pH drift method to obtain the pH_{pzc} of the as-prepared oxide systems. The dashed line applies to the system without added catalyst

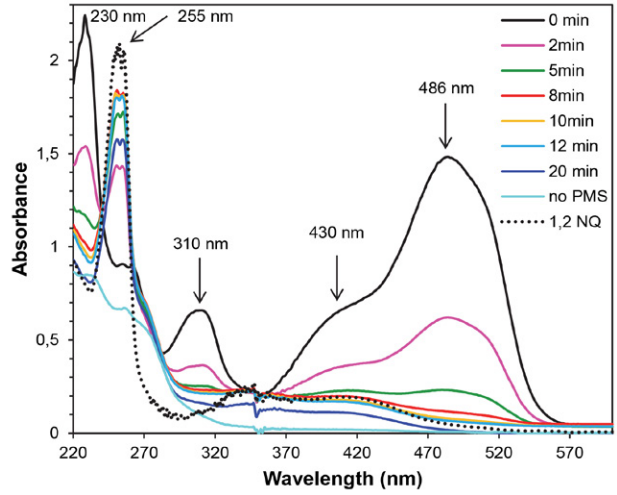

Fig. 9. UV–vis spectra of AO7 catalytic degradation on 50% Bi_2O_3-Co_3O_4. Reaction conditions: $[AO7]_o$ = 50 mg/L; [PMS]/[AO7] = 6; [Catalyst] = 0.1 g/L; initial pH = 3.04; T = 293 K.

lyst. As given in Fig. 8, the pH_{pzc} value of Co_3O_4 increased from 7.1 to 8.4 after the doping with Bi_2O_3, indicating for the enhanced content of hydroxyl groups on the surface of the composite catalyst. Such difference between the surface charge of the Co_3O_4 and Bi_2O_3-Co_3O_4 is consistent with the XPS results that show a higher content of the surface hydroxyl oxygen in the Co-Bi composite than that in Co_3O_4.

Fig. 9 depicts the UV-vis spectral changes of AO7 in solution during the catalytic degradation in the presence of most active 50% Bi_2O_3-Co_3O_4 composite. In the visible region, the spectrum of initial AO7 solution exhibits a main band with a maximum located at 486 nm and a shoulder at 430 nm, corresponding to the n–π* transitions of the hydrazone form and azo form of the dye, respectively, and are due to the chromophore-containing azo-linkage.[46] The other two bands in the ultraviolet region, located at 230 and 310 nm, are ascribed to the π–π* transitions in the benzene and naphthalene rings of AO7, respectively. It is apparent that the major band at 486 nm declined rapidly as the reaction progressed and finally disappeared after 12 min, indicating the facile break-up of the azo-linkage. In parallel, the intensity of the absorbance bands in the UV region is also reduced, implying for concomitant destruction of the conjugated p-system of the dye molecule. Meanwhile, a new absorption band around 255 nm appeared concurrently with the decay in the visible region, indicating that a new structure unit is formed from chromophore cleavage. This band was generated at the very beginning of reaction (even at 2 min) and after discoloration of the solution at 12 min, its intensity starts to drop slowly, which proves that an intermediate formed is further also degraded. 1,2-naphthoquinone was identified to contribute to the peak at 255 nm by comparing the spectra of the reaction mixture and a standard solution of 1,2-naphthoquinone.

The degradation intermediates of AO7 were also monitored by HPLC analysis. Fig. 10 shows chromatograms of the AO7 solution before and in the course of degradation catalyzed by the 50% Bi_2O_3-Co_3O_4 together with the chromatogram of a standard solution, containing the expected main intermediates from AO7 degradation. The chromatogram of the initial AO7 solution shows a single peak with a retention time t_R at 12.75 min, whose intensity dramatically declined when the reaction proceeded and almost disappeared after 10 min. Concurrently, six intermediates were generated, identified as 4-hydroxybenzenesulfonic acid (t_R at 2.6 min), phthalic anhydride (t_R at 7.08 min), phthalimide (t_R at 8.1 min), 1,2-naphthoquinone (t_R at 12.3 min), coumarin (t_R at 13.3 min), and unidentified product with t_R at 11.2 min. The intermediate product 1,2-naphthoquinone distinguished from the other ones by its highest intensity during the whole process, as well as by

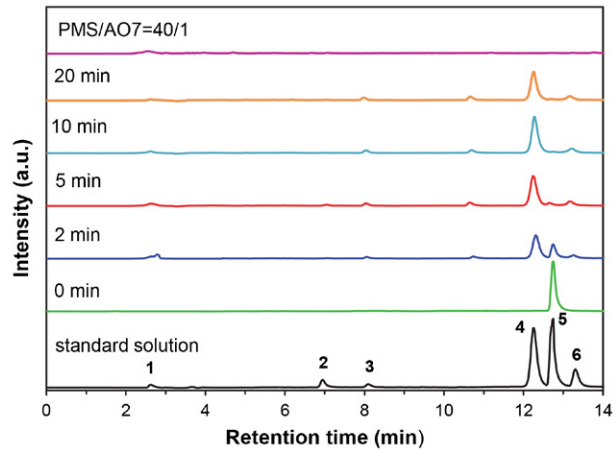

Fig. 10. HPLC chromatograms of AO7 during catalytic oxidation on 50% Bi_2O_3-Co_3O_4 and standard solution [(1) 4-hydroxybenzenesulfonic acid, (2) phthalic anhydride, (3) phthalimide, (4) 1,2-naphthoquinone, (5) AO7, (6) coumarin]. Reaction conditions: $[AO7]_o$ = 50 mg/L; [PMS]/[AO7] = 6; [Catalyst] = 0.1 g/L; initial pH = 3.04; T = 293 K.

the most well-defined intensity changes. It gradually accumulated up to 10 min and then starts to decrease as evidenced by UV-vis analysis as well. However, the disappearance of all peaks when raising the PMS/AO7 molar ratio to 40:1, corresponding to the stoichiometric one for mineralization of AO7, suggests that the generated intermediates were finally mineralized.

3. 3. Effect of Reaction Variables on AO7 Degradation

Further kinetic studies were carried out using the most active 50% Bi_2O_3-Co_3O_4 catalyst to investigate the effects of several key parameters, namely the catalyst dosage, PMS concentration, initial solution pH, and temperature on the AO7 degradation.

3. 2. 1. Effect of Catalyst Amount

Fig.11a depicts the degradation kinetics of AO7 by PMS with different Bi_2O_3-Co_3O_4 dosages in the range of 0.05 g/L – 0.3 g/L. Apparently, increasing the amount of catalyst resulted in an increased degradation rate for AO7, confirming the crucial role of the catalyst for the generation of the radicals as well as indicating that the surface reaction is the rate-limiting step. In comparison, at catalyst loading of 0.05 g/L,[3] AO7 removal efficiency could reach 100% after 20 min, whereas only 5 minutes are needed for complete dye degradation in the presence of 0.3 g/L catalyst. Accordingly, the first-order rate constant *k* increased from 0.1804 to 0.839 min^{-1} as observed in Fig 11b. Besides, the degradation rate constants present a linear trend as a function of catalyst dosage at the same PMS concentration, thereby implying that there is no competition between the dye and PMS for the active sites on the catalyst surface. The inset in Fig. 11 presenting the kinetic fitting curves confirms that the AO7 degradation follows a first-order kinetics model. The continuous increase of the AO7 degradation rate with catalyst load can be attributed to the more surface active sites for PMS activation, thereby resulting in a faster generation of reactive radical species and consequently in an enhancement of the reaction rate.

3. 2. 2. Effect of PMS Concentration

As illustrated in Fig. 12, the AO7 catalytic degradation on Bi_2O_3-Co_3O_4 also showed a positive dependence on the PMS dosage (in terms of PMS/AO7 molar ratio). At the lowest [PMS/AO7] ratio of 1:1 complete removal of AO7 was not achieved due to a lack of sufficient oxidant amount. However, as the [PMS]/[AO7] ratio was increased from 1:1 to 6:1, the AO7 removal efficiency significantly increased from 66.5% to 100% and the degradation rate constant rapidly rises from 0.113 to 0.367 min^{-1} (inset of Fig. 12). However, further increase of the [PMS]/[AO7] molar ratio to 12:1 induced only a slight enhancement in

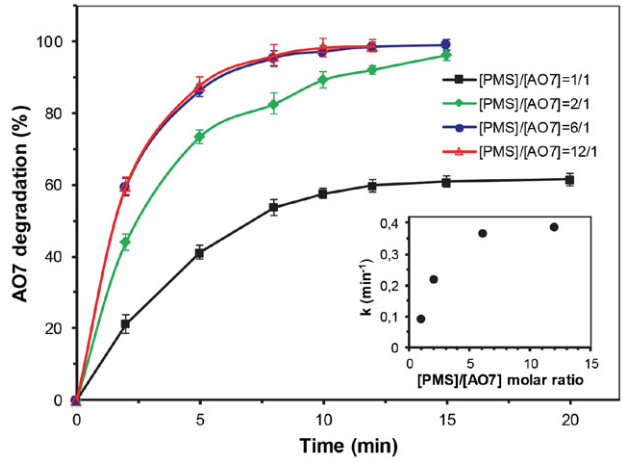

Fig. 12. Effect of PMS dosages on AO7 degradation and AO7 degradation kinetics (inset) by 50% Bi_2O_3-Co_3O_4/PMS oxidation system. Reaction conditions: 50 mg/L; [Catalyst] = 0.1 g/L; initial pH = 3.04; T = 293 K.

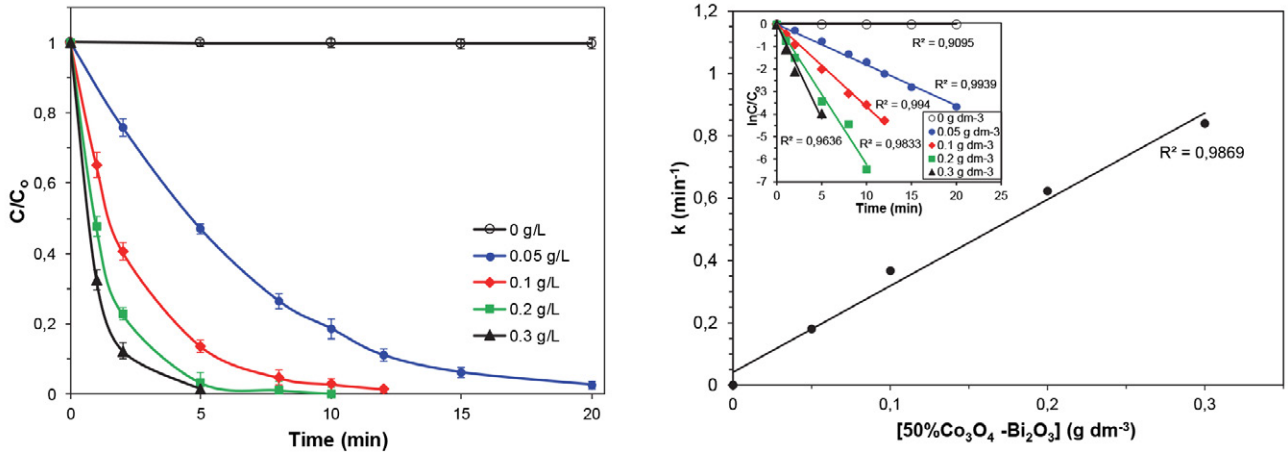

Fig. 11. Catalytic performance of 50%Bi_2O_3-Co_3O_4 at various dossages in the presence of PMS and AO7: (a) AO7 degradation; (b) AO7 degradation kinetics. Reaction conditions: $[AO7]_o$ = 50 mg/L; [PMS]/[AO7] = 6; initial pH = 3.04; T = 293 K.

the AO7 degradation rate. Being the source of active radicals, an increase of the PMS dosage promotes the generation of more radicals, which accounts for the rapid AO7 degradation. However, at high PMS concentrations, the fixed amount of catalyst gradually became the limiting factor controlling the generation of radicals so that the radical yield was almost independent of PMS dosage. Furthermore, the unreacted PMS behaves as the quencher of active radicals according to the following reactions: [47]

$$SO_4^{\cdot-} + HSO_5^- \rightarrow SO_5^{\cdot-} + HSO_4^- \quad (1)$$

$$^{\cdot}OH + HSO_5^- \rightarrow SO_5^{\cdot-} + H_2O \quad (2)$$

3. 2. 3. Effect of pH

Solution pH plays a significant role in the degradation process due to its influence on the surface charge of the catalyst as well as the existing form of PMS in solution. As the natural wastewater has variable acidity, it is important to investigate the influence of pH on the degradation efficiency of AO7 in 50% Bi_2O_3-Co_3O_4/PMS system. Fig. 13a shows that the efficient catalytic degradation of AO7 in this system is applicable to a wide pH range of 3.04 to 9.3, which covers the common pH of natural water and wastewater. Moreover, the discoloration of AO7 solution was complete in a short period of time (12 min) even at alkaline conditions. The surface of Bi_2O_3-Co_3O_4 particles is positively charged when the solution pH is less than 8.4 (pH_{pzc} of the sample). According to the pK_a values of PMS ($pK_{a1} < 0$, $pK_{a2} = 9.4$[47]), PMS mainly exists in the form of HSO_5^- in the solution pH range of 4.0 to 8.5. Therefore, PMS and catalyst surface were oppositely charged within this pH range, which facilitates their interaction through the electrostatic attractive forces. Although electrostatic repelling forces between the negatively-charged catalyst's surface and HSO_5^- are prominent at pH 9.3, slightly faster initial discoloration kinetics was observed at this pH, suggesting that base activation of PMS by NaOH (used to adjust pH to 9.3) may also take effect in basic conditions. Furthermore, the different UV-vis absorption spectrum of the solution after the degradation process at pH 9.3 imply for a different AO7 degradation mechanism (Fig. 13b). Specifically, the new peak at 255 nm did not appear in the spectra as well as a residual absorbance at 228 and 310 nm was still observed even when the reaction was completed, indicating that some intermediates generated from the fragmentation of the azo links still contain benzoic and naphthalene rings.

Meanwhile, pH variation during the AO7 degradation process was also monitored. As shown in Fig. 13c, the solution pH with an initial value of 3.04 maintained almost unchanged over time but decreased when the initial pH was 7.06 and reached around pH 3.4 within 8 min reaction. This phenomenon could be attributed to the release of protons along with PMS decomposition and the formation of acidic intermediate products during the AO7 degradation process. However, under basic conditions, the pH value only slightly decreased as the reaction went on

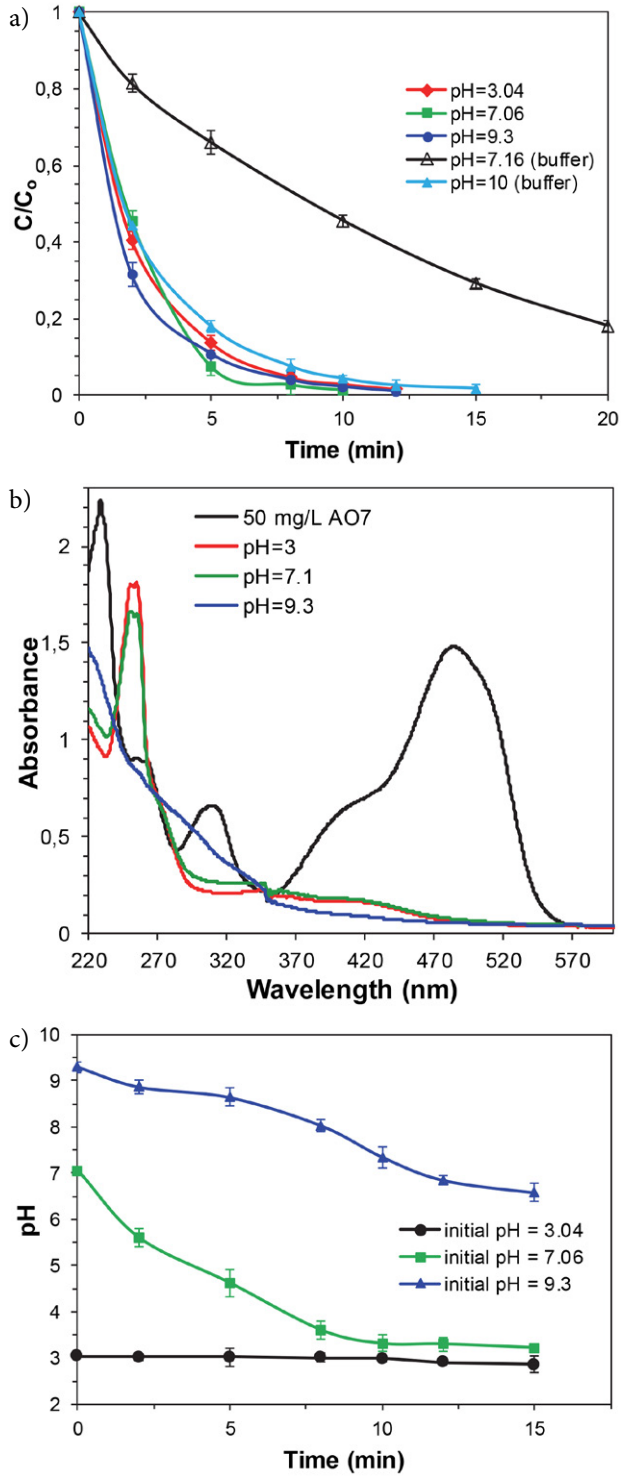

Fig. 13. Performance of 50% Bi_2O_3-Co_3O_4 for AO7 degradation with PMS at different initial pHs: (a) AO7 degradation; (b) UV–vis spectra of the AO7 aqueous solution at 12 min ; (c) Changes of pH over time in the case of different initial pH values. Reaction conditions : $[AO7]_o$ = 50 mg/L; [PMS]/[AO7] = 6; [Catalyst] = 0.1 g/L; T = 293 K.

and finally kept to nearly neutral probably due to the high initial concentration of OH^- (2.0 mM) which prevented a significant decrease in the pH.

The effect of buffer solutions on the AO7 removal efficiency was also evaluated. Accordingly with Fig. 13a, the degradation rate of AO7 was considerably decreased when the initial solution was buffered to 7.16 using 0.004 M phosphate buffer (in the forms of $H_2PO_4^-$ and HPO_4^{2-}). In the buffered system, complete AO7 degradation was achieved in 50 min and the rate constant decreased 5.3 times compared with the experiment at an initial pH of 7.06 adjusted with NaOH. The observed retarding effect could be due to the quenching of active radicals generated from PMS catalytic decomposition by phosphate anions in the solution.[48,49] In contrast, the oxidation of AO7 was quite significant when $NaHCO_3$/NaOH buffer used to adjust the initial pH to 10 (Fig. 13a). Although the surface of Bi_2O_3-Co_3O_4 is negatively charged at pH higher than 8.4 and PMS existed mostly in the form of SO_5^{2-} at pH range of 9.5–10.5, the AO7 degradation rate and efficiency were comparable to that attained in an acidic medium. Therefore, it could be speculated that along with heterogeneous activation of PMS, the active species may also be generated as a result of anion decomposition of PMS which, due to its unsymmetric structure, can easily be attacked by nucleophile such as HCO_3^-.[50] Besides, base activation of PMS by NaOH was also enhanced at pH 10.

3. 2. 4. Effect of Temperature

The effect of reaction temperature on PMS activation by 50%Bi_2O_3-Co_3O_4 for AO7 degradation was also studied. Considering the observations in Fig. 14, an increase in temperature had a positive effect on AO7 removal rate due to accelerating the decomposition of PMS into active radicals under thermal activation.[51] As the temperature increased from 18 to 38 °C, the decolorization kinetics was remarkably enhanced and the rate constant value increased from 0.283 to 0.530 min^{-1}. At 18 °C, AO7 was completely destroyed within 15 min, whereas removal reached up to 100% at 38 °C in just 7 min. The temperature dependence of the rate constant was further used to determine activation energy (E_a) by plotting ln$k$ against $1/T$ according to the Arrhenius equation (inset of Fig. 14). The calculated E_a value for AO7 degradation with 50% Bi_2O_3-Co_3O_4 as a catalyst was 22.7kJ mol^{-1}, whereas that obtained in the presence of pristine Co_3O_4 was 35.5kJ mol^{-1}. Both E_a values are higher than the activation energy of diffusion-controlled reactions (10–13 kJ mol^{-1}), revealing that the AO7 catalytic degradation process was controlled by the rate of chemical reaction on the catalyst surface rather than mass transfer rate. The lower E_a value obtained for the 50% Bi_2O_3-Co_3O_4 /PMS system was in agreement with its best AO7 degradation efficiency and confirmed that Bi_2O_3 had a great influence on the Co_3O_4 catalytic reactivity for PMS activation.

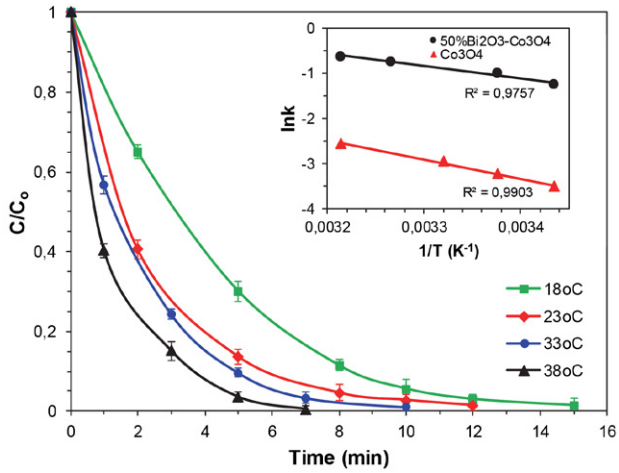

Fig. 14. Effect of reaction temperature on AO7 degradation by 50% Bi_2O_3-Co_3O_4/PMS oxidation system. Reaction conditions: $[AO7]_o$ = 50 mg/L; [PMS]/[AO7] = 6; [Catalyst] = 0.1 g/L; initial pH = 3.04.

3. 2. 5. Identification of Reactive Species

Selective radical quenching tests were performed to identify the dominating radical species formed during PMS activation by the catalyst and accounting for the AO7 degradation. The activation of PMS by metal-containing catalysts might produce sulfate ($SO_4^{\bullet-}$), hydroxyl (•OH), and peroxy-sulfate ($SO_5^{\bullet-}$) radicals.[52] The AO7 degradation by $SO_5^{\bullet-}$ could be neglected because of its much lower oxidation potential (E^o = 0.81 V).[53]

Various radical scavengers were tested in the reaction solution including ethanol (EtOH), tert-butyl alcohol (TBA), KI, and ascorbic acid and the results are presented in Fig. 15. With the addition of 0.02 M ascorbic acid, the degradation of AO7 is almost completely inhibited and the degradation rate is the same as observed by the removal of dye without PMS. Since the ascorbic acid is considered to be a strong radical scavenger, it can be concluded that the radical pathway mechanism of AO7 degradation is involved in the 50% Bi_2O_3-Co_3O_4 activated PMS system. To evaluate the contribution of $SO_4^{\bullet-}$ and •OH to AO7 degradation, EtOH and TBA were used as radical scavengers. EtOH (containing α-hydrogen) can readily react with both radicals at high and comparable rates ($k_{\bullet OH}$:1.2–2.8 × 10^9 mol L^{-1} s^{-1}; $k_{SO4\bullet-}$:1.6–7.7 × 10^7 mol L^{-1} s^{-1}), whereas the scavenging of •OH by TBA (without a-hydrogen) is much faster than $SO_4^{\bullet-}$ ($k_{\bullet OH}$:3.8–7.6 × 10^8 mol L^{-1} s^{-1}; $k_{SO4\bullet-}$:4–9.1 × 10^5 mol L^{-1} s^{-1}).[14,53,54] As observed in Fig. 15, the AO7 removal kinetics was slightly affected by the presence of TBA, and the kinetic constant of AO7 degradation decreased from 0.367 min^{-1} (with no scavenger) to 0.271 min^{-1} at a TBA/PMS ratio of 2000/1. On the other hand, the addition of EtOH resulted in decreasing AO7 removal to 76.4% at 12 min and reaching final removal efficiency of 85.2% at 20 min when the PMS was exhausted. Accordingly, around a 3-fold decrease of the reaction rate constant value was observed due to the inhibitory effect of ethanol.

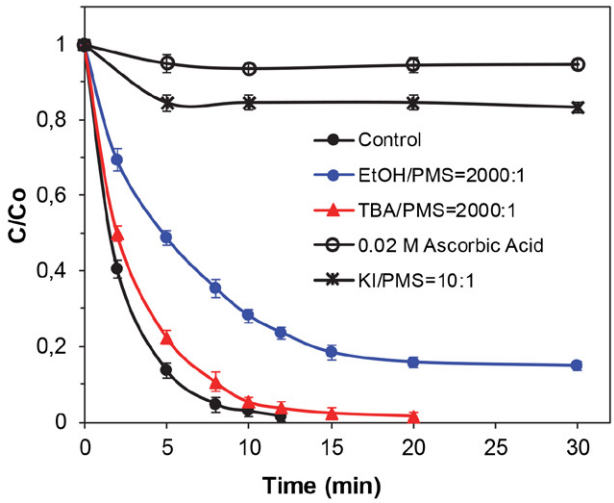

Fig. 15. Effect of radical scavengers on AO7 degradation. Reaction conditions: $[AO7]_o$ = 50 mg/L; [PMS]/[AO7] = 6; [Catalyst] = 0.1 g/L; initial pH = 3.04; T = 293 K.

These results suggest that in the Bi_2O_3-Co_3O_4/PMS system the major radical species involved in the attack of AO7 are sulfate radicals. A probable reason for the relative slight inhibitory effects of both alcohols might be that EtOH and TBA being highly hydrophilic prefer to quench free radicals in solution rather than reacting radicals in catalyst surface.[55] Furthermore, a complete suppression of the AO7 degradation was observed upon the addition of KI even at a KI/PMS ratio of 10/1. Since iodine ions are considered as scavenging agents for surface-bound radicals in advanced oxidation processes, it may be concluded that $SO_4^{\bullet-}$ radicals on the surface play a dominant role in the AO7 degradation in Bi_2O_3-Co_3O_4 /PMS oxidation system.

4. Conclusions

In this work, Bi_2O_3-Co_3O_4 composites with different content were synthesized using a facile co-precipitation method and applied as catalysts for the degradation of AO7 dye by activating PMS via a radical pathway. The XRD and HRTM characterization confirmed the coexistence of Bi_2O_3 and Co_3O_4 phases in the Bi_2O_3-Co_3O_4 composites. Compared to bare Co_3O_4, the as-prepared composite catalysts exhibited superior performance in the heterogeneous activation of PMS to generate radical species and thus induced the rapid degradation of AO7 over a wide pH range (pH 3-10). In the presence of the most active 50 wt.% Bi_2O_3-Co_3O_4, an initial AO7 concentration of 50 mg/L was completely removed within 12 min, and the rate constant is around 9.5 – fold as compared with bare Co_3O_4. The enhanced PMS-activating ability of the Bi_2O_3-Co_3O_4 composites was attributed to the increased hydroxyl oxygen content on their surface due to the presence of basic Bi oxide, which facilitates the formation of surface Co-OH complexes and promotes the activation of PMS. The increase of catalyst dosage, PMS concentration and temperature leads to enhancement of the AO7 removal efficiency, however increasing the catalyst loading is most beneficial. Based on the chemical scavenger study, sulfate radicals were identified as the major reactive species formed by the catalyst/PMS interaction and responsible for AO7 degradation. The synthesized catalytic systems could be regarded as promising heterogeneous catalysts for the degradation of organic pollutants in water through a sulfate radical approach.

Acknowledgements

Authors gratefully acknowledge financial support by the Centre for Competence»Personalized Innovative Medicine, PERIMED (EU Programme "Science and Education for Smart Growth" grant BG05M2OP001-1.002-0005-C01).

5. References

1. B. D. Tony, D. Goyal, S. Khanna, *Int. Biodeter. Biodegr.* **2009**, *63*, 462–469. **DOI:**10.1016/j.ibiod.2009.01.003
2. R. D. Ambashta, M. Sillanpää, *J. Hazard. Mater.* **2010**, *180*, 38–49. **DOI:**10.1016/j.jhazmat.2010.04.105
3. S. Eftekthari, A. Habibi-Yangjeh, Sh. Sohrabnezhad, *J. Hazard. Mater.* **2010**, *178*, 349–355. **DOI:**10.1016/j.jhazmat.2010.01.086
4. R. D. Ambashta and M. Sillanpaa, *J. Hazard. Mater.*, **2010**, *180*, 38–49. **DOI:**10.1016/j.jhazmat.2010.04.105
5. S. H. Chen, J. Zhang, C. L. Zhang, Q. Y. Yue, Y. Li and C. Li, *Desalination*, **2010**, *252*, 149–156. **DOI:**10.1016/j.desal.2009.10.010
6. M. Cai, J. Su, G. Lian, X. Wei, C. Dong, H. Zhang, M. Jin, Z. Wei, *Ultrason. Sonochem.* **2016**, *31*, 193–200. **DOI:**10.1016/j.ultsonch.2015.12.017
7. N. Riaz, F. K. Chong, B. K. Dutta, Z. B. Man, M. S. Khan, E. Nurlaela, *Chem. Eng. J.* **2012**, *185–186*, 108–119. **DOI:**10.1016/j.cej.2012.01.052
8. N. Inchaurrondo, J. Font, C. P. Ramos, P. Haure, *Appl. Catal. B: Environ.* **2016**, *181*, 481–494. **DOI:**10.1016/j.apcatb.2015.08.022
9. G. P. Anipsitakis, D.D. Dionysiou, *Environ. Sci. Technol.* **2003**, *37*, 4790–4797. **DOI:**10.1021/es0263792
10. Q. Yang, H. Choi, Y. Chen, D. D. Dionysiou, *Appl. Catal. B: Environ.* **2008**, *77*, 300–307. **DOI:**10.1016/j.apcatb.2007.07.020
11. H. Liang, H. Sun, A. Patel, P. Shukla, Z. H. Zhu, Sh. Wang, *Appl. Catal. B: Environ.* **2012,** *127*, 330–335. **DOI:**10.1016/j.apcatb.2012.09.001
11. Y. B. Ding, L. H. Zhu, N. Wang, H. Tang, *Appl. Catal. B: Environ.* **2013**, *129*, 153–162. **DOI:**10.1016/j.apcatb.2012.09.015
12. G. Nie, J. Huang, Y. Hu, Y. Ding, X. Han, H. Tang, *Chin. J. Catal.* 2017, 38, 227–239. **DOI:**10.1016/S1872-2067(16)62566-4
13. X. Dong, B. Ren, Z. Sun, Ch. Li, X. Zhang, M. Kong, S. Zheng,

D. D. Dionysiou, *Appl. Catal. B: Environ.* **2019**, *253*, 2016 – 217. **DOI:**10.1016/j.apcatb.2019.04.052
14. G. P. Anipsitakis, D. D. Dionysiou, *Environ. Sci. Technol.*, **2004**, 38, 3705–3712. **DOI:**10.1021/es035121o
15. J. Deng, S. Feng, X. Ma, Ch. Tan, Sh. Zhou, J. Li, *Sep. Purif. Technol.*, **2016**, 167, 181–189. **DOI:**10.1016/j.seppur.2016.04.035
16. J. Deng, S. Feng, K. Zhang, J. Li, H. Wang, T. Zhang, X. Ma, *Chem. Eng. J.* **2017**, *308*, 505–515. **DOI:**10.1016/j.cej.2016.09.075
17. S. N. Su, W. L. Guo, C. L. Yi, Y. Leng, Zh. Ma, *Ultrason. Sonochem.* **2012**, *19*, 469–474. **DOI:**10.1016/j.ultsonch.2011.10.005
18. J. Liu, J. Zhou, Z. Ding, Z. Zhao, X. Xu, Z. Fang, *Ultrason. Sonochem.* **2017**, *34*, 953–959. **DOI:**10.1016/j.ultsonch.2016.08.005
19. X. Y. Lou, L. X. Wu, Y. G. Guo, C. Chen, Z. Wang, D. Xiao, C. Fang, J. Liu, J. Zhao, S. Lu, *Chemosphere* 117 (2014) 582–585. **DOI:**10.1016/j.chemosphere.2014.09.046
20. K. H. Chan, W. Chu, *Water Res.* **2009**, *43*, 2513–2521. **DOI:**10.1016/j.watres.2009.02.029
21. O. S. Furman, A. L. Teel, R. J. Watts, *Environ. Sci. Technol.*, **2010**, 44, 6423–6428. **DOI:**10.1021/es1013714
22. C. D. Qi, X. T. Liu, J. Ma, C. Y. Lin, X. W. Li, H. J. Zhang, *Chemosphere*, **2016**, *151*, 280–288. **DOI:**10.1016/j.chemosphere.2016.02.089
23. B.-T. Zhang, Y. Zhang, Y. Teng, M. Fan, *Crit. Rev. Environ. Sci. Technol.* **2015**, *45*, 1756–1800.
24. G. P. Anipsitakis, E. Stathatos, D. D. Dionysiou, *J. Phys. Chem. B* **2005**, *109*, 13052–13055. **DOI:**10.1021/jp052166y
25. Y. Wang, L. Zhou, X. Duan, H. Sun, E. L. Tin, W. Jin, S. Wang, *Catal. Today* **2015**, *258*, 576–584. **DOI:**10.1016/j.cattod.2014.12.020
26. E. Saputra, S. Muhammad, H. Sun, H-M. Ang, M. O. Tade´, S. Wang, *J Colloid Interface Sci* **2013**, *407*, 467–473. **DOI:**10.1016/j.jcis.2013.06.061
27. W. Guo, S. Su, C. Yi, Z. Ma, *Environ. Prog. Sustain.* **2013**, *32*, 193–197. **DOI:**10.1002/ep.10633
28. X. Chen, J. Chen, X. Qiao, D. Wang, X. Cai, *Appl. Catal. B: Environ.* **2008**, *80*, 116–121. **DOI:**10.1016/j.apcatb.2007.11.009
29. B.-T. Zhang, Y. Zhang, W. Xiang, Y. Teng, Y. Wang, *Chem. Res. Chin. Univ.* **2017**, *33 (5)*, 822–827. **DOI:**10.1007/s40242-017-6413-6
30. W. Zhang, H. L. Tay, S. S. Lim, Y. S. Wang, Z. Y. Zhong, R. Xu, *Appl. Catal. B: Environ.* **2010**, *95*, 93–99. **DOI:**10.1016/j.apcatb.2009.12.014
31. Q. Yang, H. Choi, D. D. Dionysiou, *Appl. Catal. B: Environ.* **2007**, *74*, 170–178. **DOI:**10.1016/j.apcatb.2007.02.001
32. P. R. Shukla, Sh. Wang, H. Sun, H. M. Ang, M. O. Tadé, *Appl. Catal. B: Environ.* **2010**, *100*, 529–534. **DOI:**10.1016/j.apcatb.2010.09.006
33. P. R. Shukla, H. Sun, S.B. Wang, H. M. Ang, M. O. Tade´, *Sep. Purif. Technol.*, **2011**, 77, 230–236. **DOI:**10.1016/j.seppur.2010.12.011
34. L. Hu, X. Yang, S. Dang, *Appl. Catal. B: Environ.* **2011**, *102*, 19–26. **DOI:**10.1016/j.apcatb.2010.11.019
35. B.-T. Zhang, Y. Zhang, Y. Teng, Appl. Surf. Sci. **2018**, *452*, 443–450. **DOI:**10.1016/j.apsusc.2018.05.065
36. P. Shi, R. Su, F. Wan, M. Zhu, D. Li, S. Xua, *Appl. Catal. B: Environ.* **2012**, *123-124*, 265–272. **DOI:**10.1016/j.apcatb.2012.04.043
37. M. Kosmulski, *Adv. Colloid Interface Sci.* **2009**, *152*, 14–25. **DOI:**10.1016/j.cis.2009.08.003
38. L. Hu, G. Zhang, M. Liu, Q. Wang, P. Wang *Chem. Eng. J.* **2018**, *338*, 300–310. **DOI:**10.1016/j.cej.2018.01.016
39. M.V. Lopez-Ramon, F. Stoeckli, C. Moreno-Castilla, F. Carrasco-Marin *Carbon* **1999**, *37*, 1215–1221. **DOI:**10.1016/S0008-6223(98)00317-0
40. Z. S. Wu, W. C. Ren, L. Wen, L. Gao, J. Zhao, Z. Chen, G. Zhou, F. Li, H.-M. Cheng, *ACS Nano* **2010**, *4 (6)*, 3187–3194. **DOI:**10.1021/nn100740x
41. Z. Ai, Y. Huang, S. Lee, L. Zhang, *J. Alloys Compd.* **2011**, *509*, 2044–2049. **DOI:**10.1016/j.jallcom.2010.10.132
42. T. Tsoncheva, L. Ivanova, J. Rosenholm, M. Linden, *Appl. Catal. B: Environ.* **2009**, *89*, 365–374. **DOI:**10.1016/j.apcatb.2008.12.015
43. J. Yang, H. Liu, W. N. Martens, R. L. Frost, *J. Phys. Chem. C* **2010**, *114*, 111–119. **DOI:**10.1021/jp908548f
44. H. T. Fan, S. S. Pan, X. M. Teng, C. Ye, G. H. Li, L. D. Zhang, *Thin Solid Films* **2006**, *513*, 142–147. **DOI:**10.1016/j.tsf.2006.01.074
45. B. Y. Bai, H. Arandiyan, J. H. Li, *Appl. Catal. B: Environ.* **2013**, *142–143*, 677–683. **DOI:**10.1016/j.apcatb.2013.05.056
46. M. Stylidi, D. I. Kondarides, X. E. Verykios, *Appl. Catal. B: Environ.* **2004**, *47*, 189–201.
47. Y. H. Guan, J. Ma, X. C. Li, J. Y. Fang, L. W. Chen, *Environ. Sci. Technol.* **2011,** *45*, (21), 9308–9314. **DOI:**10.1021/es2017363
48. W. D. Oh, Z. Dong, T. T. Lim, *Appl. Catal. B: Environ.* **2016**, *194*, 169–201. **DOI:**10.1016/j.apcatb.2016.04.003
49. P. Hu, M. Long, *Appl. Catal. B: Environ.* **2016**, *181*, 103–117. **DOI:**10.1016/j.apcatb.2015.07.024
50. S. Yang, P. Wang, X. Yang, L. Shan, W. Zhang, X. Shao, R. Niu, *J. Hazard. Mater.* **2010**, *179*, 552–558. **DOI:**10.1016/j.jhazmat.2010.03.039
51. Y. J. Yao, Y. M. Cai, G. D. Wu, F. Wei, X. Li, H. hen, S. Wang, *J. Hazard. Mater.* **2015**, *296*, 128–137. **DOI:**10.1016/j.jhazmat.2015.04.014
52. G. P. Anipsitakis, D. D. Dionysiou, *Appl. Catal. B: Environ.* **2004**, *54*, 155–163. **DOI:**10.1016/j.apcatb.2004.05.025
53. P. Neta, R .E. Huie, A. B. Ross, *J. Phys. Chem. Ref. Data* **1988**, *17*, 1027–1284. **DOI:**10.1063/1.555808
54. Y. Yao, H. Chen, C. Lian, F. Wei, D. Zhang, G. Wu, B. Chen, S. Wang, *J. Hazard. Mater.* **2016**, *314*, 129–139. **DOI:**10.1016/j.jhazmat.2016.03.089
55. Y. Xu, J. Ai, H. Zhang, *J. Hazard. Mater.* **2016**, *309*, 87–96. **DOI:**10.1016/j.jhazmat.2016.01.023

Povzetek

V tej študiji smo pripravili sestavljene okside Bi_2O_3-Co_3O_4 in ocenili njihovo katalitično učinkovitost za aktiviranje peroksimonosulfata (PMS) proti razgradnji barvila Acid Orange 7 (AO7). Karakterizacijo sintetiziranih katalizatorjev smo izvedli z analizami XRD, TEM, XPS, FT-IR in ICP-OES. Povečana bazičnost hibridov Bi_2O_3-Co_3O_4 je prispevala k veliko boljši katalitični aktivnosti pri aktivaciji PMS, kar je povzročilo znatno višjo stopnjo razgradnje AO7 v primerjavi s tisto, ki jo dobimo s samim Co_3O_4. Vzorec s 50 mas. % Bi_2O_3 je pokazal najboljše rezultate v širokem območju pH z zelo majhnim uhajanjem Co (72 μg/L) tudi v kislih pogojih. Razgradnja 50 mg/L AO7 je dosegla skoraj 100 % v kratkem času (12 minut) z uporabo zelo nizke koncentracije katalizatorjev (0,1 g/L) in z razmerjem [PMS]/[AO7] = 6. Proučevali smo vpliv vsebnosti Bi_2O_3, količine katalizatorja, molskega razmerja [PMS]/[AO7], začetnega pH in temperature na razgradnjo AO7. S poskusi na osnovi kaljenja radikalov so bili površinsko vezani sulfatni ostanki, ki nastajajo v oksidacijskem sistemu Bi_2O_3-Co_3O_4/PMS, dokazani kot prevladujoča vrsta radikalov.